

## Magnetic and Optical Properties of Rb and Cs Clusters Incorporated into Zeolite A\*

Truong Cong Duan,<sup>†</sup> Takehito Nakano, and Yasuo Nozue*Department of Physics, Graduate School of Science,  
Osaka University, Toyonaka, Osaka 560-0043, Japan*

(Received 20 November 2006; Accepted 29 December 2006; Published 15 January 2007)

Optical and magnetic properties are studied on Rb and Cs clusters incorporated into the cages of aluminosilicate zeolite A (structure type code LTA), where  $\alpha$  and  $\beta$  cages with inside diameters of  $\sim 1.1$  and  $\sim 0.7$  nm, respectively, are arrayed in a simple cubic structure. The average number of guest alkali atoms per  $\alpha$  cage,  $n$ , was changed from dilute loading to  $\sim 5$  and  $\sim 3.5$  for Rb and Cs, respectively. At  $n > 2$ , the absorption coefficient at mid-infrared region increases significantly. This is assigned to a contribution of the Drude term in a metallic phase. The change from insulating phase to the metallic one is ascribed to a wider bandwidth of the  $1p$  state of clusters compared with that of the  $1s$  state. All samples show Curie-Weiss law with negative Weiss temperatures. In Rb clusters, both of the Curie constant and the absolute value of Weiss temperature gradually increases with increasing  $n$  at  $n > 2$ , and ferromagnetic properties are clearly found at  $n > 4$ . This  $n$ -dependence is essentially different from that in ferromagnetism in K clusters at  $n > 2$ . Cs clusters shows quite small values of Curie constant at  $n > 2$  and also non-ferromagnetic behavior up to the maximum value of  $n$ . [DOI: 10.1380/ejssnt.2007.6]

Keywords: Magnetic measurements; Alkali metals; Zeolites; Clusters; Metal-insulator transition; Ferromagnetic properties

## I. INTRODUCTION

Alkali-metal clusters with mutual interaction can be generated by the loading of guest alkali atoms into the cages of zeolite crystals. Magnetically ordered states have been found in periodically arrayed alkali metal clusters in zeolites, such as a ferromagnetism in K clusters in zeolite A [1], an antiferromagnetism in Na clusters in sodalite [2] and a ferrimagnetism in K clusters in low silica X zeolite [3]. They are quite novel magnetic materials, because they contain no magnetic elements and also the magnetically ordered states are realized by the mutual interaction of  $s$ -electrons confined in the clusters.

Zeolite A is one of aluminosilicate zeolites with the framework type code of LTA. The LTA structure is constructed of  $\beta$  cages and  $\alpha$  cages, as shown in Fig. 1, where inside diameters of  $\beta$  and  $\alpha$  cages are  $\sim 0.7$  and  $\sim 1.1$  nm, respectively. Both cages are arrayed in a simple cubic structure. The framework ( $\text{Al}_{12}\text{Si}_{12}\text{O}_{48}$ ) is negatively charged, and exchangeable alkali cations, such as  $\text{Na}^+$ ,  $\text{K}^+$  and  $\text{Rb}^+$ , are distributed in the space of the framework for charge neutrality. Typical sites of cations are also shown in Fig. 1, where indicated sites are at the centers of six- and eight-rings. These sites have the cation occupancy of 100%. Other sites, such as those beside four-ring (not shown in the figure), has low occupancy rate. When guest K atoms are loaded into K-type zeolite A (chemical formula:  $\text{K}_{12}\text{Al}_{12}\text{Si}_{12}\text{O}_{48}$ ), the guest  $4s$ -electrons are shared among several  $\text{K}^+$  ions and cationic K clusters are formed in the  $\alpha$  cage [4]. The origin of the spontaneous magnetization in K clusters in zeolite A has been assigned to a spin-cant mechanism of antiferromagnet [5]. This material has been assigned to a Mott insulator because the Urbach tail absorption is observed at the infrared region [6]. A Mott insulator of this material is explained by the large Coulomb repulsion energy between  $s$ -electrons con-

finned in the cluster and a narrow energy bandwidth. If we change the alkali element from K to heavier ones, such as Rb and Cs, the confinement potential of  $s$ -electrons in the cluster may become shallower than that in K cluster due to the decrease in the ionization energy. This may result in the larger electron-transfer energy  $t$  between adjacent clusters which results in a wider energy bandwidth. The increase in  $t$  is expected to strongly affect the electronic properties.

In previous papers [7, 8], ferromagnetic properties have been also found when Rb is loaded into partly Rb-exchanged zeolite A with the chemical formula of  $\text{K}_{6.5}\text{Rb}_{5.5}\text{Al}_{12}\text{Si}_{12}\text{O}_{48}$ , where K cations partially remained unexchanged. The observed ferromagnetism was, however, found to be quite incomplete, and attributed to an effect of the residual  $\text{K}^+$  ions [8]. In highly Rb-exchanged zeolite A ( $\text{K}_1\text{Rb}_{11}\text{Al}_{12}\text{Si}_{12}\text{O}_{48}$ ), the structure of Rb-loaded samples are reported to have a tentative space group of  $F\bar{4}3c$  with some disorder and show paramagnetic properties even at 2 K [9]. In the present paper, we prepared carefully a highly Rb-ion exchanged zeolite A in order to investigate Rb-rich clusters in detail. We newly find a clear ferromagnetic phase transition at certain Rb-loading densities. We also prepared Cs clusters in zeolite A and investigated their magnetic and optical properties.

## II. EXPERIMENTAL PROCEDURE

We used a powder of Na-type zeolite A ( $\text{Na}_{12}\text{Al}_{12}\text{Si}_{12}\text{O}_{48}$ ) provided by Tosoh Co. Ltd., as a starting material. This zeolite is abbreviated as Na-LTA hereafter. The crystal size is a few microns. We exchanged the  $\text{Na}^+$  ions to  $\text{K}^+$ ,  $\text{Rb}^+$  and  $\text{Cs}^+$  ones step by step by soaking zeolite powder to aqueous solutions of KCl, RbCl and CsCl at  $80^\circ\text{C}$ . The products used in this study were confirmed to have chemical formulas of  $\text{Rb}_{10.8}\text{K}_{1.2}\text{Al}_{12}\text{Si}_{12}\text{O}_{48}$  and  $\text{Cs}_8\text{Rb}_1\text{K}_1\text{H}_2\text{Al}_{12}\text{Si}_{12}\text{O}_{48}$  by inductively coupled plasma (ICP) spectrometry for K, Rb and Al atoms and by atomic absorption spectrometry (AAS) for Cs atom. These compounds are denoted as

\*This paper was presented at Handai Nanoscience and Nanotechnology International Symposium (Handai Nano 2006), Osaka University, Japan, 20-22 November, 2006.

<sup>†</sup>Corresponding author: duan@nano.phys.sci.osaka-u.ac.jp

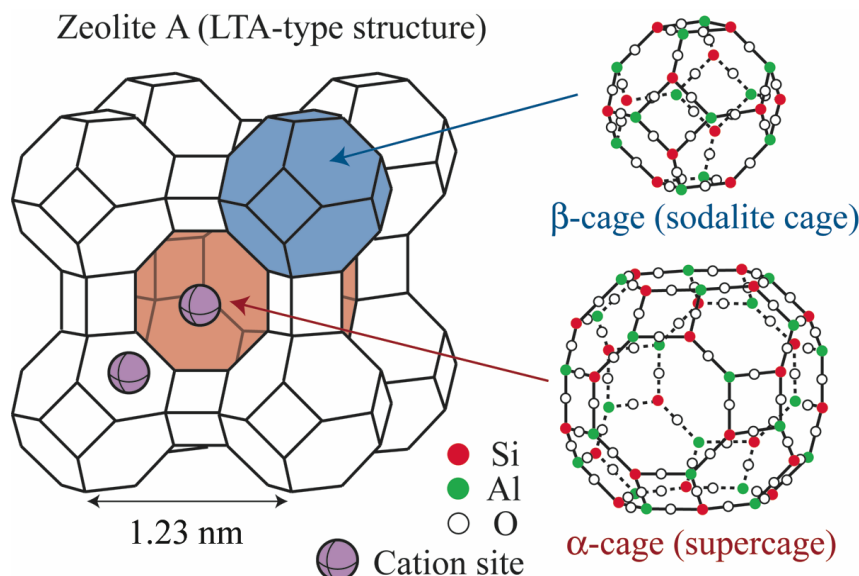


FIG. 1: Schematic illustration of the framework structure of aluminosilicate zeolite A (LTA-type structure). There are two different cages,  $\alpha$ - and  $\beta$ -one. Typical alkali cation sites are also shown, where equivalent sites are neglected.

Rb-LTA and Cs-LTA, hereafter.

Rb-LTA and Cs-LTA were fully dehydrated at 500°C in high vacuum for one day. Pure Rb metal was adsorbed into Rb-LTA at a several different loading densities at 150°C in a quartz glass tube. After the loading of Rb metal, the samples were heated at 150°C for more than 1 week with stirring many times in order to obtain homogeneous loading. The average number of guest Rb atoms per  $\alpha$  cage,  $n$ , was changed from 0 to  $\sim 5$ , where  $n \sim 5$  corresponds to the nearly saturated value. Hence, the chemical formula of the Rb-loaded Rb-LTA is given as  $K_{1.2}Rb_{10.8+n}Al_{12}Si_{12}O_{48}$ . The value of  $n$  is equal to the average number of  $s$ -electrons per  $\alpha$  cage. The Rb-loaded Rb-LTA is denoted as Rb/Rb-LTA, hereafter. The Cs-loaded Cs-LTA, which is denoted as Cs/Cs-LTA hereafter, is also prepared with similar procedure at a several different loading densities. The maximum loading density,  $n$ , was  $\sim 3.5$ .

Since all samples are extremely air-sensitive, measurements were performed with the samples sealed in quartz glass tubes with pure He gas except for the mid-infrared optical measurement as shown below. Diffuse reflection spectra were measured at room temperature by using a UV-VIS-NIR spectrometer (Cary 5G, Varian) and an FTIR system (MAGNA 550, Nicolet). The former is available for the photon energy range of 0.5 - 6.0 eV; the latter is for 0.3 - 1 eV with the sample sealed in a quartz glass tube. In order to extend the spectral range to lower energy, we used a sample-sealing holder with KBr windows. By using this holder, we obtained the diffuse reflectivity down to 0.05 eV with the FTIR system. The optical absorption spectrum was obtained from diffuse reflectivity,  $r$ , by the Kubelka-Munk transformation  $(1-r)^2/2r^2$  [10]. The sum spectrum of the reflectivity and transmittance,  $R+T$ , was obtained from that of diffuse reflectivity,  $r$ , by using the equation  $R+T = 4r/(1+r)^2$  [4]. The DC magnetization was measured by using a SQUID magnetometer (MPMS-XL, Quantum Design) with temperature

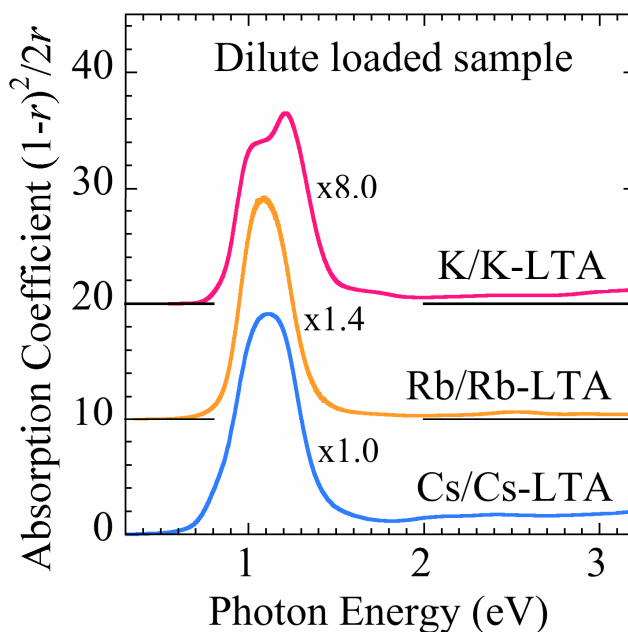


FIG. 2: The optical absorption spectra of K, Rb and Cs clusters in zeolite A with dilute loading density.

range of 1.8-300 K and external magnetic field up to 5 T.

### III. RESULTS AND DISCUSSION

#### A. Optical properties

Figure 2 shows the absorption spectra of dilutely loaded Rb/Rb-LTA and Cs/Cs-LTA at room temperature. The spectrum of K/K-LTA is also plotted for comparison. Spectra of Rb/Rb-LTA and Cs/Cs-LTA show clearly a

strong absorption peak at the photon energy of  $\sim 1.1$  eV, similar to that of K/K-LTA. The strong absorption in K/K-LTA has been explained as follows [4]. The  $4s$ -electron of the guest K atom is attracted by  $K^+$  ions in the cage, but is repulsed by the negatively charged zeolite-framework. Then, the  $4s$ -electron is shared by several  $K^+$  ions and confined in the cage. If we assume a spherical well potential formed in the  $\alpha$  cage, quantum electronic states of  $1s$ ,  $1p$ ,  $1d$ ,  $2s$ , and so on, appear. When the diameter of the spherical well is set to the inside diameter of the  $\alpha$  cage, 1.1 nm, the energy difference between  $1s$  and  $1p$  states is calculated as 1.2 eV. Therefore, the observed strong absorption peaks at  $\sim 1.2$  eV is assigned to the excitation of  $s$ -electron in  $1s$  state to  $1p$  one. In the present samples of Rb/Rb-LTA and Cs/Cs-LTA, similar interpretation can be applied; namely, the  $5s$  and  $6s$  electrons of the guest Rb and Cs atoms are shared by several  $Rb^+$  and  $Cs^+$  ions, respectively, in the  $\alpha$  cage, and form respective clusters there. The energies of quantum states of Rb and Cs clusters are determined by the inside diameter of  $\alpha$  cage. Hence, their absorption peaks are observed at the energy similar to that in K cluster.

The absorption peak of K/K-LTA has a doublet structure. The absorption peak in Rb/Rb-LTA and Cs/Cs-LTA, however, does not split into doublet structure, as seen in Fig. 2. Spectral width is slightly narrower than that of K/K-LTA. The origin of the doublet structure in K/K-LTA was assigned to a band effect under the assumption of metallic phase [4]. The latest study, however, shows that K clusters are in the insulating phase. Hence,  $s$ -electrons in dilutely generated K-clusters are localized in each cage and absorption spectrum reflects quantum states of  $s$ -electron in cluster. Average structure of present material has a cubic symmetry, but the occupancy at some cation sites is less than 100%. For example, an  $\alpha$  cage with one guest alkali atom contains 13 cations. The eight and three cations fully occupy major sites at the centers of six- and eight-rings, respectively. These 11 cations can have a cubic symmetry. Remaining two cations are expected to occupy partly 12 sites at the side of four-ring. Hence, the distribution of 13 cations in  $\alpha$  cage cannot have a cubic symmetry. This may lead to a splitting of  $1p$  state. Therefore, the doublet structure of absorption peaks in K/K-LTA can be ascribed to the splitting of  $1p$  state. The electronic potentials of Rb and Cs atoms are shallower than that of K. Hence, the splitting of  $1p$ -state in Rb and Cs clusters may be smaller than that of K cluster. Then, spectral splitting becomes narrower as giving a single peak.

At higher loading densities in K/K-LTA, reflectance peaks have been observed at 0.8-1.2 eV at  $n > 0.4$ , and they are assigned basically to the  $1s$ - $1p$  transition [4]. At  $n > 2$ , new peaks have been observed at 1.5 eV and 2.0 eV. They are assigned to the  $1p$ - $1d$  transition with the surface plasmon effect [4]. In the present samples of Rb/Rb-LTA and Cs/Cs-LTA, the reflectance spectra are basically similar to that of K/K-LTA but a significant difference is observed in the surface plasmon effect. In K clusters the oscillator strength of peak at 2.0 eV increases with increasing loading density  $n$  and becomes much larger than unity at higher K-loading densities [4]. This peak is due to the collective motion of  $s$ -electrons well-confined in clusters and called the surface plasmon effect. In Rb and Cs

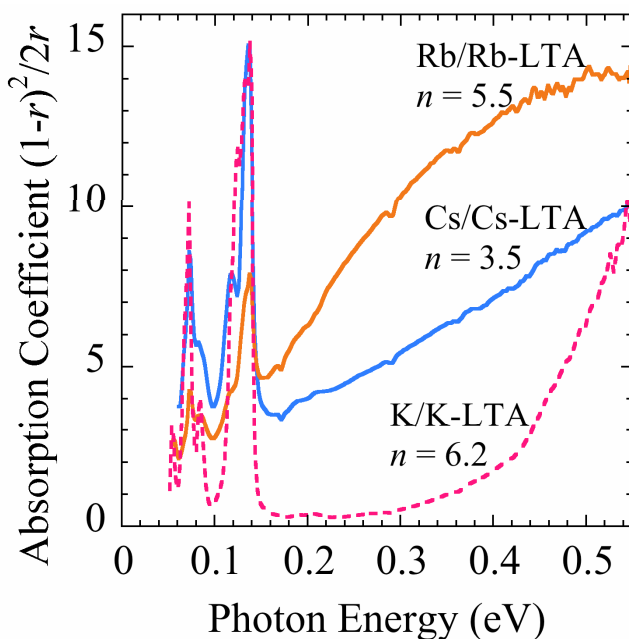


FIG. 3: The infrared absorption spectra of K, Rb and Cs clusters in zeolite A. The respective loading densities are  $\sim 6.2$ ,  $\sim 5$  and  $\sim 3.5$ .

clusters, we did not observe such a significant concentration of the oscillator strength. As mentioned above, when we change alkali metal from K to Rb and Cs, the confinement potential of  $s$ -electrons in the cluster becomes shallower and, as a result,  $s$ -electrons in the excited state can spill out to adjacent clusters. Such delocalization nature of guest electrons is thought to be the clear reason for the disappearance of surface plasmon effect in Rb- and Cs-clusters.

In the infrared region, we found a significant difference in optical properties of Rb/Rb-LTA and Cs/Cs-LTA compared to that of K/K-LTA. Figure 3 shows the infrared absorption spectra for Rb and Cs clusters in zeolite A at nearly saturated loading density, *i.e.*  $n \sim 5$  for Rb cluster and  $\sim 3.5$  for Cs one. The data of K clusters ( $n = 6.2$ ) is also plotted for comparison (dashed line). The finite contribution of normal reflection at the surface of powder particles cannot be completely neglected in highly loaded Rb/Rb-LTA and Cs/Cs-LTA. In this case, an absorption coefficient obtained from the Kubelka-Munk transformation of the diffuse reflectance has less accuracy. In the present paper, however, we do not go into detail of this problem, but the spectral difference with K/K-LTA is obvious. In K/K-LTA, the absorption coefficient exponentially decreases with decreasing the photon energy. This Urbach tail absorption is a typical shape of insulator [11]. The many sharp peaks at lower energies can be assigned to the contribution of phonon excitation of zeolite framework [12]. Also in the Rb and Cs clusters, the absorption coefficient decreases with decreasing the photon energy, but still has large values at 0.05 eV. The increase in the absorption at low energy can be assigned to the decreases in the absorption gap or the contribution of Drude term in a metallic state. This increase in the absorption at mid-infrared region suddenly occurs at  $n > 2$ . Therefore,

these phenomena can be attributed to the  $1p$  states of the cluster. Rb and Cs have lower ionization energy than that of K atom. Hence, the electron confinement potential of these clusters may become shallower than that of K cluster. Then, the electron transfer energy between adjacent clusters in  $\alpha$  cages increases through the 8-rings, resulting in the much wider bandwidth of the  $1p$  state. At present, we do not have direct evidence in conductivity data, but the samples of Rb/Rb-LTA and Cs/Cs-LTA are plausibly in a metallic phase at  $n > 2$ .

## B. Magnetic properties

### 1. $n$ -dependence of magnetic properties

Data is not shown here, but magnetic susceptibility of Rb and Cs clusters at  $n \leq 2$  shows the Curie-Weiss law with negative Weiss temperature, indicating an antiferromagnetic coupling between magnetic moments of clusters. No magnetic phase transition is observed down to 2 K at  $n \leq 2$ . The Weiss temperature,  $T_W$ , and the Curie constant,  $C$ , systematically vary depending on the number of electrons per cage,  $n$ , and they have a maximum value at  $n \sim 1$ . According to the ideal model without any inhomogeneity, the loading density of  $n = 1$  corresponds to the just-half-filled electron concentration of  $1s$  states. As mentioned above, the samples with  $n \leq 2$  are assigned to insulator from the optical spectra. Hence, each cluster may have a localized magnetic moment with  $s = 1/2$  in a Mott insulating phase. When  $n$  deviates from unity, the number of spin-singlet clusters with zero or two  $s$ -electrons increases, which leads to the decrease in  $C$ . Furthermore, the mutual interaction between magnetic clusters is disconnected by the spin-singlet clusters, results in the decrease in  $|T_W|$ . Hence,  $C$  and  $|T_W|$  can have the maximum at  $n = 1$ .

On the other hand, at  $n > 2$ , the magnetic properties of Rb and Cs clusters are clearly different from each other. Figure 4 shows temperature dependence of the reciprocal of magnetic susceptibility,  $\chi$ , for Rb and Cs clusters in zeolite A with different loading densities.

In Rb clusters with  $n \sim 3.5$  and  $\sim 5$ ,  $\chi$  obeys the Curie-Weiss law with negative Weiss temperature. The values of  $C$  and  $|T_W|$  gradually increase with increasing  $n$  at  $2 < n \leq 5$ , and  $C$  and  $T_W$  reach to  $2.97 \times 10^{-4}$  K emu/cm<sup>3</sup> and  $-18$  K, respectively, at  $n \sim 5$ . If we assume the  $g$  value of 2, the Curie constant at the full occupation of  $\alpha$  cage with  $s = 1/2$  magnetic moment amounts to  $C_0 = 3.35 \times 10^{-4}$  K emu/cm<sup>3</sup>. The observed value at  $n \sim 5$  is almost equal to this value. The rather large negative  $T_W$  indicates a strong antiferromagnetic coupling between magnetic moments of Rb clusters. This sample shows ferromagnetic properties at low temperatures, as shown in the next section. In K clusters in zeolite A,  $C$  shows a rapid increase at  $n > 2$ , and keeps nearly constant value of  $\sim 3 \times 10^{-4}$  K emu/cm<sup>3</sup> [6]. The observed maximum value of  $C$  in Rb clusters is similar to that in K clusters, but the  $n$ -dependence is quite different.

As seen in Fig. 4, Cs clusters at  $n \sim 3.5$  also show the Curie-Weiss law with slightly negative Weiss temperature,  $T_W = -1.5 \pm 0.5$  K. The Curie constant, however, shows very small value  $\sim 0.65 \times 10^{-4}$  K emu/cm<sup>3</sup>. This value

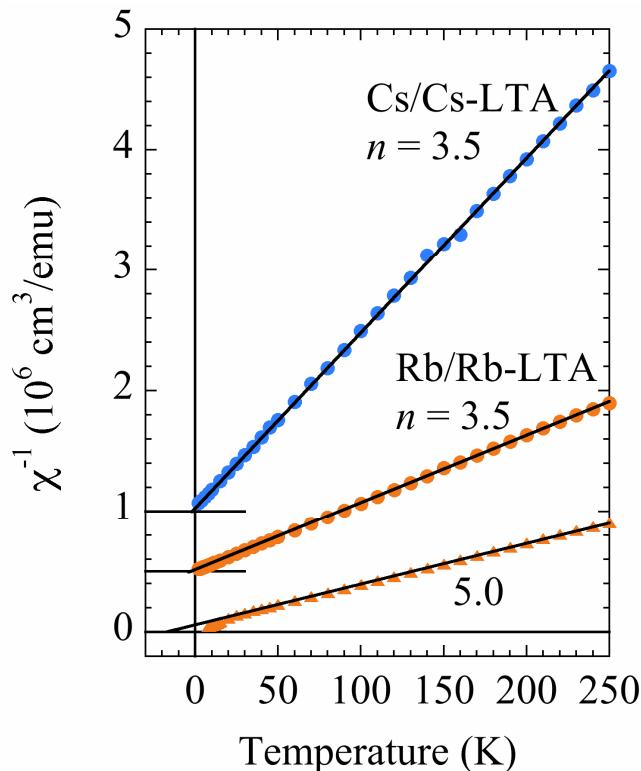


FIG. 4: Temperature dependence of the reciprocal of magnetic susceptibility of Rb and Cs clusters in zeolite A. Magnetic susceptibility,  $\chi$ , is obtained by using formula  $\chi = (M_{3T} - M_{1T})/\Delta H$ ,  $\Delta H = 2$  T, where  $M_{3T}$  and  $M_{1T}$  are the magnetization measured at 3 and 1 T, respectively, in order to eliminate a contribution from a very small amount of ferromagnetic impurities whose signal survives even at room temperature.

is only  $\sim 0.2C_0$ . The values of  $C$  and  $T_W$  are found to be almost  $n$ -independent at  $2 < n \leq 3.5$ . These results indicate that the number of localized magnetic moments is quite small and it seems that there is almost no magnetic interaction between them in Cs clusters. According to the optical spectra, Cs clusters at  $n > 2$  may be in a metallic phase. Therefore, the significant decrease in the effective localized magnetic moments as well as the decrease in the magnetic interaction may be explained by the metallic phase.

### 2. Ferromagnetic properties in Rb clusters in zeolite A

Figure 5 shows the temperature dependence of magnetization,  $M$ , for Rb/Rb-LTA measured at 10 Oe [13]. At  $n \sim 4.0$ , magnetization only shows paramagnetic behavior down to 1.8 K. At  $n \sim 4.4$ , however,  $M$  suddenly increases around 2 K corresponding to the ferromagnetic phase transition. With increasing  $n$ , the Curie temperature,  $T_C$ , as well as the value of  $M$  at low temperature increases and reaches to  $T_C = 5$  K and  $M = 0.20$  G for the nearly saturated loading sample with  $n = 5.0$ . The ferromagnetic phase transition is confirmed by the Arrott plot analysis of magnetization curves, and the value  $T_C$  is estimated [13]. Data is not shown here, but hysteresis

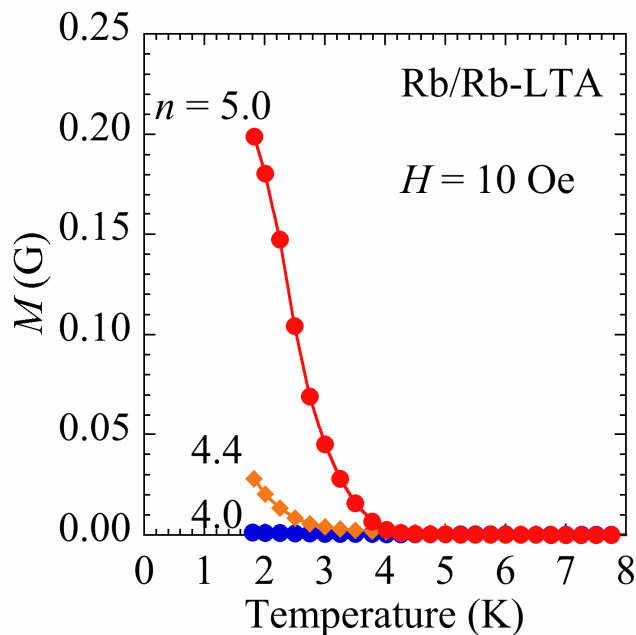


FIG. 5: Temperature dependence of magnetization of Rb clusters in zeolite A measured under the magnetic field of 10 Oe at several loading densities of  $n$  [13].

loop is clearly observed in the magnetization curve at low temperature, although it is not observed in K clusters in zeolite A [1]. The value of  $M = 0.2$  G corresponds to the magnetization of  $0.04\mu_B$  per cage, which is much smaller than the average localized moment estimated from the Curie-Weiss law at higher temperatures.

In the present paper, we discuss a possible mechanism of the ferromagnetism. As mentioned in the previous section, these samples show negative values of  $T_W$ , indicating that the antiferromagnetic interaction exists between magnetic moments of Rb clusters. Hence, the ferromagnetic magnetization may not be ascribed to an ordinary ferromagnetism. There are two possible origins of the coexistence of the spontaneous magnetization and the antiferromagnetic coupling. The first candidate is the spin-canting mechanism of antiferromagnet as in K clusters in K-LTA [5]. In K clusters, spontaneous magnetization is suddenly observed when  $n$  exceeds 2, where the  $s$ -electrons start to occupy  $1p$ -state [5]. The orbital degeneracy of  $1p$ -state is responsible for the construction of spin-canting mechanism [5]. The second candidate is a ferrimagnetism. Recently, N-type ferrimagnetism is found in K clusters in low silica X (LSX) zeolite [3]. This sample is assigned to be metallic. A model of ferrimagnetism

is proposed to be constructed of non-equivalent magnetic-sublattices of K clusters in  $\beta$  cages and supercages in LSX zeolite [3]. In Rb clusters in the present work, ferromagnetic properties are observed only at  $n > 4$ , and the  $n$ -dependence of magnetic property is essentially different from that in K clusters. This result indicates that the degeneracy of the  $1p$ -state may not play an essential role in Rb clusters. Moreover, the ferromagnetism in K clusters is realized in an insulating phase, whereas that in Rb clusters possibly in a metallic phase. Hence, the origin of the spontaneous magnetization in Rb clusters may be different from that in K clusters in zeolite A. As for a ferrimagnetism, non-equivalent magnetic sublattices should be considered. According to the optical spectra shown in Fig. 2, Rb clusters are formed in the  $\alpha$  cage at low loading densities. At higher loading densities, however, some electrons might be trapped in the  $\beta$  cages as well. If the itinerant ferromagnetism is realized in the magnetic sublattice of  $\alpha$  cages, a ferrimagnetism can be explained by the antiferromagnetic coupling between the ferromagnetic sublattice of  $\alpha$  cages and localized magnetic moments in  $\beta$  cages. At present stage, we have no direct evidence of this model. Further investigations are needed to clarify the mechanism of ferromagnetism in Rb clusters.

#### IV. SUMMARY

We have prepared Rb and Cs clusters in zeolite A and investigated their magnetic and optical properties. At loading density  $n < 2$ , Rb and Cs clusters are in an insulating state. A large absorption coefficient is observed at mid-infrared region in both Rb and Cs clusters at  $n > 2$ . This may be due to the Drude term of a metallic state, indicating that a metal-insulator transition is induced by doping to the  $1p$ -states. The magnetic properties are found to show systematic changes depending on  $n$ . A new ferromagnetic phase is clearly observed in Rb clusters for  $n > 4.0$ . Possible origins for the ferromagnetism are discussed.

#### Acknowledgments

We thank Mr. S. Tamiya for the chemical analysis of zeolites. This work has been partially supported by Grant-in-Aid for Creative Scientific Research (15GS0213), MEXT of Japan, and also by the 21st Century COE Program named: "Towards a new basic science: depth and synthesis".

- [1] Y. Nozue, T. Kodaira, and T. Goto, *Phys. Rev. Lett.* **68**, 3789 (1992).  
 [2] V. I. Srdanov, G. D. Stucky, E. Lippmaa, and G. Engelhardt, *Phys. Rev. Lett.* **80**, 2249 (1998).  
 [3] T. Nakano, K. Goto, I. Watanabe, F. L. Pratt, Y. Ikemoto, and Y. Nozue, *Physica B* **374-375**, 21 (2006).  
 [4] T. Kodaira, Y. Nozue, S. Ohwashi, T. Goto, and O. Terasaki, *Phys. Rev. B* **48**, 12245 (1993).

- [5] T. Nakano, Y. Ikemoto, and Y. Nozue, *Physica B* **281/282**, 688 (2000).  
 [6] T. Nakano, Y. Ikemoto, and Y. Nozue, *Eur. Phys. J. D* **9**, 505 (1999).  
 [7] Y. Nozue, T. Kodaira, S. Ohwashi, N. Togashi, and O. Terasaki, *Surf. Rev. Lett.* **3**, 701 (1996).  
 [8] T. Nakano, Y. Ikemoto, and Y. Nozue, *J. Mag. Mag. Mat.* **226-230**, 238 (2001).

- [9] T. Ikeda and T. Kodaira, *Stud. Surf. Sci. Catal.* **135**, 300 (2001).
- [10] P. Kubelka and Z. Munk, *Z. Tech. Phys.* **12**, 593 (1931).
- [11] F. Urbach, *Phys. Rev.* **92**, 1324 (1954).
- [12] I. E. Maxwell and A. Baks, in: *The influence of exchangeable cations on zeolite framework vibrations*, Molecular sieves, Advances in chemistry series 121, Eds. W. M. Meier and J. B. Vythoeven (USA, Washington DC, (1973) p. 87.
- [13] T. C. Duan, T. Nakano, and Y. Nozue, *J. Mag. Mag. Mat.*, in press.